Appendix to "Enhanced ordering of interacting filaments by molecular motors"

Pavel Kraikivski, Reinhard Lipowsky, and Jan Kierfeld

Max Planck Institute of Colloids and Interfaces, Science Park Golm, 14424 Potsdam, Germany

(Dated: May 24, 2006)

In this Appendix we present details of the simulation model. Our microscopic model for motility assays describes filament configurations, motor heads, and polymeric motor tails as separate degrees of freedom. One end of the motor tail is anchored to the substrate, and the motor head on the other end can bind to a filament in the correct orientation due to the tail flexibility. The motion of the motor head along the filament stretches the polymeric motor tail, which gives rise to a loading force acting both on the motor head and the attached filament. Accordingly our model is completely defined by specifying (i) the filament dynamics arising from all forces and torques acting on each filament which originate from attached motors, the steric repulsion with other filaments and thermal noise, (ii) the response of the polymeric motor tail to stretching, (iii) the dynamics of a motor head bound to a filament, and (iv) rules for the attachment of motors to filaments.

Filament equations of motion. Filaments follow an overdamped dynamics for translation and rotation with thermal noise and external forces and torques from the stretched motor tails of attached motors and the repulsive filament-filament interaction. We consider N rigid filaments of length L (with index $i = 1, ..., N$). The configuration of filament i on the planar substrate is specified by the two-dimensional vector $\mathbf{r}_i$ for its center of mass and by the angle θ_i or the unit vector $\mathbf{u}_i = (\cos\theta_i, \sin\theta_i)$ for its orientation, see Fig. 1.

The filament is subject to forces $\mathbf{F}_i^\alpha$ from N_i attached motors (with index $\alpha = 1, ..., N_i$). Each such force arises from stretching the polymeric tail of motor α. In addition to motor forces, the filaments are subject to interaction forces $\mathbf{F}_{ij}$ due to the repulsive interactions between filaments i and j. Both motor and interaction forces give
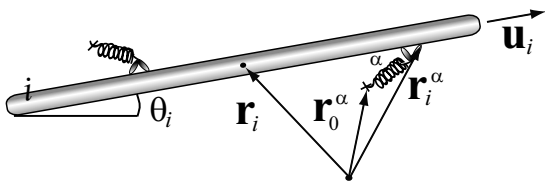

FIG. 1: Schematic top view of a filament i with two motors attached. $\mathbf{r}_i$ is the filament's center of mass, θ_i and $\mathbf{u}_i$ its orientational angle and unit vector, respectively. The attached motor α is anchored at $\mathbf{r}_0^\alpha$, and its head is positioned at $\mathbf{r}_i^\alpha$.

rise to corresponding torques $\mathbf{M}_i^\alpha$ and $\mathbf{M}_{ij}$. In the planar geometry all torque vectors are parallel to the direction perpendicular to the plane. Both forces and torques are described in detail in the following two sections.

The equations for an overdamped translational and rotational motion are

$$\boldsymbol{\Gamma} \cdot \partial_t \mathbf{r}_i = \sum_{\alpha=1}^{N_i} \mathbf{F}_i^\alpha + \sum_{j=1}^{N} \mathbf{F}_{ij} + \boldsymbol{\zeta}_i \qquad (1)$$

$$\Gamma_\theta \partial_t \theta_i = \sum_{\alpha=1}^{N_i} M_i^\alpha + \sum_{j=1}^{N} M_{ij} + \zeta_{\theta,i} \qquad (2)$$

where $\boldsymbol{\Gamma}$ is the matrix of translational friction coefficients,

$$\boldsymbol{\Gamma} = \Gamma_\parallel \mathbf{u}_i \otimes \mathbf{u}_i + \Gamma_\perp (\mathbf{I} - \mathbf{u}_i \otimes \mathbf{u}_i) \qquad (3)$$

($\mathbf{I}$ is the unit matrix and $\otimes$ the dyadic vector product) and Γ_θ is the rotational friction coefficient. The translational friction coefficients are given by $\Gamma_\perp = 2\Gamma_\parallel = 4\pi\eta L/\ln(L/D)$, where η is the viscosity of the surrounding liquid, and the rotational friction coefficient is $\Gamma_\theta = \Gamma_\parallel L^2/6$ [1]. $\boldsymbol{\zeta}_i(t)$ are the Gaussian distributed thermal random forces and $\zeta_{\theta,i}(t)$ is a Gaussian distributed thermal random torque with correlations $\langle \boldsymbol{\zeta}_i(t) \otimes \boldsymbol{\zeta}_j(t') \rangle = 2T\mathbf{T}\delta_{ij}\delta(t-t')$ and $\langle \zeta_{\theta,i}(t)\zeta_{\theta,j}(t') \rangle = 2T\Gamma_\theta\delta_{ij}\delta(t-t')$, respectively.

Interaction forces and torques. Because hard-core interactions give rise to singular force contributions as soon as two filaments of diameter D overlap, we use a purely repulsive short-range interactions in the simulation. The forces between two filaments are calculated by discretizing each filament into $M = L/D$ beads with their centers at positions $\mathbf{r}_{a,i}$ (with index $a = 1, ..., M$). In the simulation we choose $M = 40$ Any two beads a and b on different filaments $i \neq j$ have a repulsive interaction $U(|\mathbf{r}_{a,i} - \mathbf{r}_{b,j}|)$ $(a, b = 1, ..., M)$ of finite range r_r,

$$\begin{aligned} U(r) &= U_0 \left(\frac{D^2}{(r - 3D/4)^2} - \frac{D^2}{r^2} \right) & \text{for } r < r_r \\ &= 0 & \text{for } r > r_r \end{aligned} \qquad (4)$$

This interaction potential diverges at a bead distance $r = 3D/4$ and the energy scale U_0 is chosen such that beads do not come closer than D during the simulation, such that it approximates a hard-core interaction. As the maximal force exerted by a filament is $F_{st}L/\langle d_m \rangle$, where $\langle d_m \rangle \sim 1/\sigma w$ is the mean distance between bound motors we typically have to choose a value $U_0/D \sim F_{st}\sigma w L$ for a motor density σ and a capture radius ℓ_m. Summing
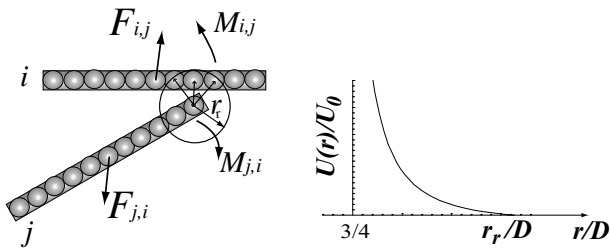
FIG. 2: Left: Schematic top view of two interacting filaments i and j, which are discretized into $M = L/D$ beads. r_r is the range of the interaction between beads. Right: Bead interaction potential $U(r)/U_0$ as a function of r/D.
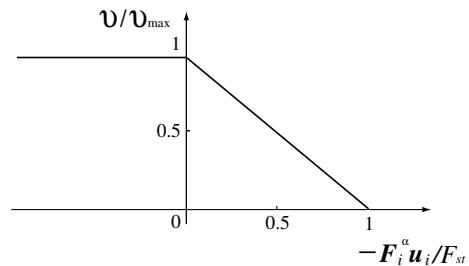

FIG. 3: Force-velocity relation of motor heads. For $F_i^\alpha \cdot \mathbf{u_i} \geq 0$ the head moves with maximal velocity $v = v_{\max}$. For $F_i^\alpha \cdot \mathbf{u_i} < 0$ the motor head is pulled backwards and the velocity decreases linearly. If the projected pulling force exceeds the stall force F_{st}, i.e., for $F_i^\alpha \cdot \mathbf{u_i} < -F_{st}$ the motor head stops, $v = 0$.

over all beads of two filaments gives the interaction forces and torques

$$\mathbf{F}_{ij} = -\sum_{a=1}^{M}\sum_{b=1}^{M} U'(|\mathbf{r}_{ai,bj}|)\frac{\mathbf{r}_{ai,bj}}{|\mathbf{r}_{ai,bj}|} \tag{5}$$

$$\mathbf{M}_{ij} = -\sum_{a=1}^{M}\sum_{b=1}^{M} U'(|\mathbf{r}_{ai,bj}|)\frac{\mathbf{u}_i \times \mathbf{r}_{ai,bj}}{|\mathbf{r}_{ai,bj}|}\left[\left(a-\frac{1}{2}\right)D - \frac{L}{2}\right] \tag{6}$$

where $\mathbf{r}_{ai,bj} \equiv \mathbf{r}_{a,i} - \mathbf{r}_{b,j}$ and $U'(r) = dU/dr$.

Motor forces and torques and polymeric motor tail. Each force $\mathbf{F}_i^\alpha$ arises from the polymeric tail of a motor α, which is attached to filament i and stretched by the directed motion of the motor head on the filament. $-\mathbf{F}_i^\alpha$ is the stretching force acting on the polymeric tail of motor α. The tail of motor α is anchored at $\mathbf{r}_0^\alpha$ and the position of the head on filament i is $\mathbf{r}_i^\alpha$. The end-to-end vector of the polymeric tail is $\Delta\mathbf{r}^\alpha \equiv \mathbf{r}_i^\alpha - \mathbf{r}_0^\alpha$. For simplicity, we model the polymeric tail as a freely jointed chain such that $-\mathbf{F}_i^\alpha$ is obtained by inverting the force-extension relation of a freely jointed chain in three spatial dimensions (we neglect confinement effects due to the planar substrate). Then $-\mathbf{F}_i^\alpha$ is pointing in the direction $\Delta\mathbf{r}^\alpha$ and its absolute value given by

$$|\Delta\mathbf{r}^\alpha|/L_m = f_{\mathrm{FJC}}(|\mathbf{F}_i^\alpha|b_m/T) \quad \text{with} \tag{7}$$

$$f_{\mathrm{FJC}}(x) \equiv 1/\tanh x - 1/x , \tag{8}$$

where L_m is the contour and b_m the monomer length of the polymeric motor tail. Other chain models can be implemented similarly if the force-extension relation is known, for example, semiflexible chain models [2]. In order to obtain the force as a function of the motor head position or the end-to-end vector of the motor tail the force-extension relation (7) is inverted using

$$-\mathbf{F}_i^\alpha = \frac{T}{b_m}\frac{\Delta\mathbf{r}^\alpha}{|\Delta\mathbf{r}^\alpha|}f_{\mathrm{FJC}}^{-1}(|\Delta\mathbf{r}^\alpha|/L_m) \quad \text{with} \tag{9}$$

$$f_{\mathrm{FJC}}^{-1}(y) \approx \frac{1}{1-y} - 1 + 2y , \tag{10}$$

which gives the correct limits $f_{\mathrm{FJC}}^{-1}(y) \approx 3y$ of a Gaussian chain for small extensions $y \ll 1$ and $f_{\mathrm{FJC}}^{-1}(y) \approx 1/(1-y)$ for $y \approx 1$ close to full stretching. Finally, the motor torques on the filament are given by

$$\mathbf{M}_i^\alpha = (\mathbf{r}_i^\alpha - \mathbf{r}_i) \times \mathbf{F}_i^\alpha \tag{11}$$

Motor head equation of motion. The position of the head of motor α on filament i is given by

$$\mathbf{r}_i^\alpha = \mathbf{r}_i + x_i^\alpha \mathbf{u}_i \tag{12}$$

with $|x_i^\alpha| \leq L/2$. The filament polarity is such that the motor head moves in the direction $\mathbf{u}_i$. The dynamics of the motor head is described by the deterministic equation of motion

$$\partial_t x_i^\alpha = v(\mathbf{F}_i^\alpha) \tag{13}$$

where $v = v(\mathbf{F}_i^\alpha)$ is the force-velocity relation of a motor α on a filament i with orientation $\mathbf{u}_i$. We assume a piecewise linear force-velocity relation

$$\begin{aligned} v(\mathbf{F}_i^\alpha) &= v_{\max} & \text{for } \mathbf{F}_i^\alpha \cdot \mathbf{u}_i \geq 0 \\ &= v_{\max}\left(1 - \frac{|\mathbf{F}_i^\alpha|}{F_{st}}\right) & \text{for } 0 > \mathbf{F}_i^\alpha \cdot \mathbf{u}_i > -F_{st} \\ &= 0 & \text{for } \mathbf{F}_i^\alpha \cdot \mathbf{u}_i < -F_{st} \end{aligned} \tag{14}$$

with the maximal motor velocity $v_{\max}$ and the stall force F_{st}.

Motor attachment and detachment. We assume that the motor binds to the filament when the distance between the fixed end of the motor tail at $\mathbf{r}_0^\alpha$ and the filament is smaller than a capture radius ℓ_m. Apart from the stall force F_{st} the motor is also characterized by its detachment force F_d, above which the unbinding rate of the motor head becomes large. For simplicity we assume in our model that the motor head detaches whenever the force F_i^α exceeds a threshold value F_d. We consider the case of processive motors with a high duty ratio close to unity, i.e., motors detach from a filament only if they reach the filament end or if the total force becomes larger than the detachment force F_d.
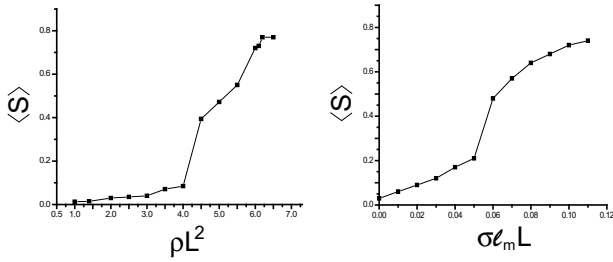
FIG. 4: Plots of the order parameter $\langle S \rangle$ crossing the isotropic-nematic transition. Left: The order parameter as a function of the dimensionless filament density ρL^2 at zero motor density. The transition point is at $\rho L^2 = 4.3$. Right: The order parameter as a function of the dimensionless motor density $\sigma \ell_m L$ for a filament density $\rho L^2 = 2$ and $L/\ell_m = 100$ (which is the same as for the snapshots in Figs. 1 and 4 of the article). The transition point is at $\sigma \ell_m L = 0.047$. In each plot we can identify the transition points as inflection points of the order parameter curve. Each data point in the order parameter plots corresponds to the average value of the order parameter taken over 10^6 time steps.

Simulation. The above equations of motion (1) and (2) for the filaments with the interaction forces (5) and torques (6) and the motor forces (9) and torques (11) completely describe the filament dynamics for a given configuration of motor heads on the filaments. The equation of motion (13) for the motor heads on a filament with the force-velocity relation (14), on the other hand, describes the dynamics of motor heads on the filaments. For the simulation these equations of motion are discretized into time steps Δt. At each time step, we update the motor head positions x_i^α according to (13) and the filament positions and orientations according to (1) and (2). Each data point in the phase diagram in Fig. 3 of the article and Fig. 4 below corresponds to simulation runs over 10^6 time steps.

We simulate a quadratic assay of size $25\mu m^2$ with periodic boundary conditions and rigid filaments of length $L = 1\mu m$ and diameter $D = L/40$ at room temperature $T \simeq 4 \times 10^{-3} pN\,\mu m$. For the viscosity of the surrounding liquid we use a value $\eta = 0.5 pN\,s/\mu m^2$. We use a maximum motor speed of $v_{max} = 1\mu m\,s^{-1}$ and a stall force of $F_{st} = 5pN$. The capture radius for motor proteins is $\ell_m = 10^{-2}\mu m$ and the length of the fully stretched motor tail $L_m = 5 \times 10^{-2}\mu m$.

Order parameter. In our simulations the phase transition between nematic and isotropic phase is characterized by time averages of the order parameter $S \equiv \sum_{i \neq j} \cos(2(\theta_i - \theta_j))/N(N-1)$. The equilibrium transition is found numerically from the inversion point of the curve $\langle S \rangle = \langle S \rangle(\rho)$ as a function of filament density or $\langle S \rangle = \langle S \rangle(\sigma)$ as a function of motor density. We find a second order isotropic-nematic transition also for non-zero motor-density, which can be seen in the additional plots for the order parameter, Fig. 4, which we include in this appendix. The transition happens around a value $\langle S \rangle \simeq 0.2$, which can therefore be used as a threshold value for active nematic ordering.

[1] M. Doi and S.F. Edwards, *The Theory of Polymer Dynamics* (Clarendon, Oxford, 1986).
[2] J. Kierfeld *et al.*, Eur. Phys. J. E **14**, 17 (2004).